NASA TECHNICAL MEMORANDUM 107640

ENVIRONMENTAL FATIGUE IN ALUMINUM-LITHIUM ALLOYS

R. S. Piascik

JULY 1992

Also published in the Proceedings of the International Workshop on Structural Integrity of Aging Airplanes, Atlanta, Georgia, March 31-April 2, 1991.

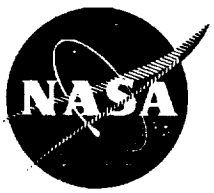

National Aeronautics and Space Administration

Langley Research Center

Hampton, Virginia 23665-5225

Environmental Fatigue In Aluminum-Lithium Alloys

Robert S. Piascik
Mechanics of Materials Branch
NASA Langley Research Center
Hampton, VA 23665-5225, USA

ABSTRACT

Aluminum-lithium alloys exhibit similar environmental fatigue crack growth characteristics compared to conventional 2000 series alloys and are more resistant to environmental fatigue compared to 7000 series alloys. The superior fatigue crack growth behavior of Al-Li alloys 2090, 2091, 8090 and 8091 is due to crack closure caused by tortuous crack path morphology and crack surface corrosion products. At high R and reduced closure, chemical environment effects are pronounced resulting in accelerated near threshold da/dN. The beneficial effects of crack closure are minimized for small cracks resulting in rapid growth rates. Limited data suggest that the "chemically small crack" effect, observed in other alloy system, is not pronounced in Al-Li alloys. Modeling of environmental fatigue in Al-Li-Cu alloys relate accelerated fatigue crack growth in moist air and salt water to hydrogen embrittlement.

INTRODUCTION

Advanced aluminum - lithium alloys are becoming commercially available for aerospace application; sheet, plate, extrusion and forgings are being produced for fixed wing aircraft and rotorcraft applications. Because Li based alloys are targeted for critical structural applications, it is important to fully understand the durability and damage tolerance capabilities of these new alloys. Environment is known to accelerate the deterioration of aircraft structure[1] and reduce component lifetime through complex environmental fatigue interactions[2]. The objective of this paper is to review the current understanding of environmental fatigue in advanced Al-Li alloys.

BACKGROUND

Research over the last decade has resulted in the development of several advanced aluminum-lithium alloys[3-6]. Table 1 lists the compositions and mechanical properties of a number of commercially available alloys in the peak aged (T8) and under aged (T351) conditions. The addition of lithium to aluminum reduces density and significantly increases stiffness; for each weight percent of Li added to aluminum (up to 4 wt. %), density and elastic modulus is improved by 3% and 4%, respectively. Designers are able to achieve a weight saving of up to 17 % by using Al-Li alloys instead of traditional aluminum alloys. Copper and magnesium (Table 1) are added to enhance solid solution and precipitate strengthening. Zirconium is added to form a fine dispersion of intermetallic phases and reduce localized deformation. The precipitation sequence for the Al-Li-X system is complex; upon aging, homogeneous precipitation of Li rich (δ'-Al_3Li), Cu bearing (T_1-Al_2CuLi, Θ'-AlLi) or Mg containing (S'-Al_2CuMg) metastable phases occur. These matrix precipitates restrict dislocation motion which greatly enhances alloy strength.

Structural applications of Al-Li-X alloys require an understanding of how microstructure affects deformation and fracture under different loading and environmental conditions. Studies of the effect of slip morphology on the monotonic and cyclic ductility of Al-Li alloys[7] and Al-Li-Cu alloys[8,9] show that ductility is controlled by strain localization which depends on the extent of work softening on the glide plane. As aging is increased from under aged to peak strength, shearable precipitates localize monotonic strain in intense bands of deformation which produce stress concentrations and reduced ductility. In peak and over aged material, precipitates are not readily sheared by mobile dislocations resulting in increased tensile strength (Table 1). Commercially available Al-Li alloys exhibit an anisotropic unrecrystallized grain structure and deformation texture that results in mechanical properties that are dependent on plate orientation [10]. Typically, strength and toughness properties are 30 to 50% lower across the plate thickness, e.g. short-longitudinal and short-transverse (S-L and S-T) orientations, compared to longitudinal and transverse properties (L and L-T). Cracks are formed by the interaction of slip bands at grain boundary ledges during tensile tests and propagate either intergranularly along precipitate free zones (PFZ's) or transgranularly dependent upon aging treatment. During cyclic deformation, cracks nucleate at slip bands that form at surface discontinuities (constituent particles, grain boundaries and pits). Fatigue cracks propagate along slip planes which promote large crack path deflections and wedging of fracture surface asperities. The fatigue crack growth characteristics of Al-Li alloys are greatly affected by these crack closure processes which are discussed in the following paragraphs.

FATIGUE CRACK PROPAGATION IN Al-Li ALLOYS

In general, Al-Li-X alloys exhibit comparable and in some cases improved fatigue crack growth resistance compared to traditional 2000 and 7000 series aluminum alloys[11,12]. However, improved fatigue crack growth resistance of lithium containing aluminum alloys is linked to crack closure. Closure is a widely studied phenomenon[13] that results in premature contact of the fatigue crack surfaces during the unloading portion of the fatigue cycle and is defined by K_{cl}, the closure stress intensity factor. Closure reduces crack tip driving force and results in slower fatigue crack growth rates, da/dN. The effect of crack closure is quantified by the effective crack tip stress intensity range factor; $\Delta K_{eff} = K_{max} - K_{cl}$, where $K_{cl} > K_{min}$. Typically, closure effects dominate at low stress intensity range and low load ratios (R).

Three mechanisms of crack closure affect the fatigue crack growth behavior of high strength aluminum alloys, see Figure 1[14]. Plasticity-induced crack closure is associated with the plastically deformed crack wake that is left by the growing fatigue crack. Presumably, the increased volume of material left on the crack wake flanks (regions of plane stress) result in premature contact of the crack surface during unloading. Crack closure also occurs as a result of crack surface roughness. Here, crack surface asperities contact during the fatigue loading cycle, lowering the crack tip driving force for crack propagation. The third form of crack closure is due to crack surface corrosion or oxide wedging. Voluminous corrosion products, oxides or fretting debris on crack surfaces prevent the crack surfaces from closing and reduce ΔK_{eff}.

Small Crack Growth

The fatigue crack growth characteristics of high strength aluminum alloys can be divided into two regimes, small (≤ 1 mm) crack and long (> 1 mm) crack growth. Because small cracks propagate faster than long cracks[15], the small crack growth regime is extremely important and must be considered separately in durability analysis or component lifetimes may be overestimated. The small crack phenomenon is of particular importance for Al-Li alloys, where fatigue crack growth resistance is greatly influenced by crack closure, a crack size dependent phenomenon.

The initiation and growth of small fatigue cracks in high strength aluminum alloys has been the subject of many studies[15,17,18]. Surface imperfections, e.g., machining marks, corrosion pits or microstructural imperfections (constituent particle, precipitate/matrix interface), are sites for fatigue crack initiation. After initiation, the rate of growth of microstructurally small fatigue cracks generally exceed those of long cracks when subjected to the same applied

ΔK. This behavior is reported when cracks are small in length compared to microstructural dimensions, small relative to the scale of crack tip plasticity, or when they are physically short.

Small fatigue crack growth behavior of commercial Al-Li 2090, 2091 and 8091 in air is shown in Figure 2. Here, surface replication, optical and electrical potential methods were used to monitor the growth rates of naturally-occurring surface cracks (2 to 1000 μm in size). For all the alloys shown in Figure 2, microcracks were found to initiate as a result of strain localization at cracked surface constituent particles, surface pits and uncracked particle/matrix interfaces. Although the data shown in Figure 2 exhibit a wide degree of scatter[1], Al-Li alloys and traditional 7150 and 2124 aluminum alloys exhibit the same general small crack growth response, suggesting that there is no apparent influence of microstructure and composition on small crack growth for different Al alloys in air environment. The majority of small crack data exhibit accelerated rates compared to long crack growth rate at low R (0.1). As the stress ratio is increased (R=0.75), closure effects are reduced for long cracks. Here, high R long crack growth rates are similar to or higher than the majority of small crack data shown in Figure 2 suggesting that much of the small crack data is affected by closure. A small proportion of small crack growth data, for $\Delta K \leq 1.5$ MPa$\sqrt{m}$, exhibit accelerated da/dN compared to high R long crack growth results. Typically, these data represent the growth of cracks less than 10 μm in size. Here, crack lengths are the approximate size of microstructural features and accelerated crack growth rates due to localized residual stress or notch effects are likely.

Long Crack Growth

Al-Li alloys (2090, 2091 and 8090) exhibit similar fatigue crack growth rates in air compared to alloy 2124 and improved rates compared to alloy 7150, see Figure 3. The reduced fatigue crack growth rates exhibited by Al-Li alloys are attributed to extremely high crack closure levels which remain significant at high ΔK, Figure 3 (insert). For alloy 2090-T81, K_{cl} ranges from 2 to 3 MPa$\sqrt{m}$ at near threshold stress intensities and remain 50% of K_{max} at high ΔK (7 to 8 MPa$\sqrt{m}$)[12]. The high closure levels exhibited by Al-Li alloys compared to conventional aluminum alloys is directly associated with a high deflected crack path caused by the predominance of {111} slip band cracking in combination with cyclic plasticity and oxide debris closure.

[1] The variation in fatigue crack growth rates for naturally-occurring micro-cracks is due to a number of factors; crack tip interaction with microstructure (grain boundaries, inclusions etc.) is known to retard da/dN[19], and the uncertainties caused by variation in crack front shape and stress concentration effects of inclusions can result in anomalous behavior.

ENVIRONMENTAL EFFECTS ON FCG

Small Crack Growth

Little is known about the environmental effects on small crack growth in aluminum alloys[15]. Based on limited gaseous environment data for a conventional aluminum alloy 7075 , enhanced fatigue crack growth rates in air relative to vacuum is due to a water vapor induced hydrogen embrittlement mechanism[20]. No such gaseous data has been obtained for Al-Li alloys. For steels, researchers have shown that small cracks (< 5 mm) exposed to salt water environment grow at a rate 300 times faster than long cracks[21]. Modeling of the "chemically" small crack phenomenon in salt water suggests that reactant and product concentrations within the occluded crack geometry are dependent on crack depth and mouth opening and thus ΔK, R, loading wave form and crack geometry[22,23]. Limited data for alloy 2090 suggest that the "chemically" small crack phenomenon does not occur in Al-Li alloys[16]. Shown in Figure 4 is the crack length (a) versus load cycle (N) result for a constant ΔK (2.9 MPa$\sqrt{m}$, R=0.75) experiment performed in salt water (1% NaCl, -0.840 V_{SCE}). Little variation in fatigue crack growth rate is observed as a function of crack length; 5.7×10^{-6} mm/cycle for 300 μm < a < 1.3 mm and 5.1×10^{-6} mm/cycle for 1.3 mm < a < 4.3 mm. Other limited comparisons, for alloys 2090 and 7075 do not support the "chemically" accelerated small crack growth hypothesis[16]. Additional research is required to fully understand the environmental effect on small fatigue crack growth behavior in aluminum alloys.

Long Crack Growth

Moist Air Environment: The effect of moist air on the fatigue crack growth characteristics of commercial Al-Li alloys, 2000 and 7000 series alloys is shown in Figure 5. The greatest environmental effect is observed at near threshold fatigue crack growth rates where both Al-Li and conventional aluminum alloys exhibit accelerated fatigue crack growth rates in moist air compared to vacuum. Based on limited data, low ΔK crack growth rates are roughly factors of 10, 100 and 150 times faster in moist air compared to vacuum for Al-Li, 2000 series and 7000 series alloys, respectively. Although these data suggest that Al-Li alloys exhibit the smallest environmental effect compared to vacuum, similar moist air rates are observed for Al-Li and 2000 series alloys. The greatest environmental sensitivity, resulting in the highest fatigue crack growth rates, is observed for 7000 series alloys in moist air. For ΔK greater than 10 MPa$\sqrt{m}$, environmental effects in these alloys are reduced; moist air and vacuum rates converge and are typically a factor of 1.5 to 3 greater than those observed in vacuum.

Crack tip hydrogen embrittlement due to the reaction of water vapor with newly created

crack tip surfaces is the likely cause of accelerated FCG in moist air[16,24,34-38]. The damaging effect of water vapor on fatigue crack propagation in alloy 2090 is shown for near threshold fatigue at high R in Figure 6[24]. For water vapor pressures below 0.2 Pa, at 5 Hz, fatigue crack growth rate is strongly dependent on H_2O pressure; fatigue crack growth rates steadily decrease as H_2O pressure is decreased until inert vacuum/helium rates are observed. A factor of ten reduction in da/dN is observed as H_2O pressure is lowered below 0.2 Pa. For H_2O pressures above 0.2 Pa, a saturation behavior is observed with the growth rate in pure water vapor equaling that of moist air. This behavior is similar to that observed for conventional alloys (7075 and 2219) exposed to pure water vapor at Paris regime crack growth rates (7 $MPa\sqrt{m} \leq \Delta K \leq 15.5\ MPa\sqrt{m}$) and where accelerated da/dN is explained by a transport controlled mechanism[36]. At low water vapor pressures, environmental fatigue damage is H_2O transport limited due to rapid crack surface chemical reactions. Here, Knudsen impeded molecular flow is insufficient to sustain crack tip H_2O pressures. Mechanistically, accelerated da/dN in water vapor is due to hydrogen produced by the dissociation of H_2O at the crack tip. Adsorbed atomic hydrogen is thought to be transported, possibly by mobile dislocations, to an embrittled region ahead of the crack tip [37,38].

Molecular oxygen, does not accelerate fatigue crack growth in alloy 2090. Equal fatigue crack growth rates for oxygen, helium and vacuum, shown in Figure 7, demonstrate that oxygen is not damaging. The lack of an O_2 effect on da/dN suggests that the crack tip surface oxide film does not increase fatigue damage preventing reversible slip[24]. These results further suggest that accelerated fatigue crack growth rates observed in air are primarily caused by the damaging effect of hydrogen producing water vapor.

Salt Water Environment: Studies have shown that the rate of fatigue crack propagation in high strength aluminum alloys is accelerated by salt water environments. The magnitude of the corrosion fatigue effect depends on a variety of material, environment and loading variables[39].

Shown in Figure 8 is a wide variation in corrosion fatigue crack growth characteristics for alloy 8090 in salt water (3.5% NaCl solution) at high and low R fatigue loading[40]. At high R=0.7, 8090 fatigue crack growth rates are rapid and similar to those observed for alloy 2024 exposed to salt water. The results in Figure 8 also reveal that 8090 environmental fatigue crack growth rates are greatly reduced at R = 0.1. Alloy 8090 corrosion fatigue crack growth rates are reduced compared to alloy 2024 and are reduced compared to 8090 fatigue crack growth rates in the less aggressive moist air environment (Figure 3). Closure is thought to cause the slow corrosion fatigue crack growth rates observed at R = 0.1. Fractography of the low R

fatigue fracture surface revealed a tortuous crack path and copious amounts of corrosion/fretting debris. These results suggest that decreased corrosion fatigue crack growth behavior of 8090 in salt water at low R is due to crack closure caused by surface roughness and corrosion product debris. These results highlight the large effect of environment and closure on fatigue crack growth characteristics in Al-Li alloys.

The effect of salt water (1% NaCl solution) environment on near threshold (high R) fatigue crack growth in alloy 2090 was studied by performing experiments under controlled anodic potential, see Figure 9[24]. In salt water, alloy 2090 near threshold FCG rates are a factor of 15 greater than inert helium rates. At high ΔK (15 MPa$\sqrt{m}$), the effect of environment is greatly reduced. At identical anodic potentials, alloy 2090 exhibits decreased crack growth rates compared to alloy 7075. Anodic potentials enhance crack tip oxidation reactions which result in metal ion hydrolysis, lowered pH and increased crack tip hydrogen production by proton reduction. Aluminum hydrolysis is thought to be the major reaction which lowers crack tip pH leading to increased crack tip hydrogen and accelerated fatigue crack growth rates.

Mild cathodic potential reduces high R corrosion fatigue crack growth rates compared to anodic crack growth rates[24]. The beneficial effect of cathodic potential is examined in Figure 10. At low ΔK (2.2 MPa$\sqrt{m}$, R=0.8) and anodic polarization (-0.840 V_{SCE}), a constant crack growth rate is maintained to a crack length of 2.1 mm. Here, a cathodic potential (-1.240 V_{SCE}) was applied, resulting in crack arrest. At 10^6 load cycles, a potential of -0.840 V_{SCE} was again applied. An additional 2.2 million cycles (over 76 hours exposure) elapsed before crack growth resumed, achieving a steady state rate similar to the initial anodic condition. A second polarization of -1.240 V_{SCE} reproduced crack arrest. It is speculated that crack growth retardation and arrest during cathodic polarization is due to a surface film effect, possibly hydroxide based. The fact that nearly 2 million load cycles are required before anodic rates are resumed suggest that mechanical damage is needed to penetrate the cathodically formed surface film. The crack tip surface film may act to protect the crack tip, possibly inhibiting the formation of crack tip hydrogen or acting as a barrier to hydrogen transport. Additional electrochemical studies directed at the effect of anodic and cathodic potential on Al-Li alloy crack tip chemistry, surface film properties and hydrogen production are required to assist in understanding of crack tip damage mechanisms during corrosion fatigue.

MODELING OF CORROSION FATIGUE CRACK GROWTH

Complex changes in the log da/dN - log ΔK behavior of Al-Li-Cu alloy are related to environmentally induced changes in fracture mode[37,38]. Table 2 correlates the fatigue crack

growth characteristics of alloy 2090 in inert, moist air and salt water environments with fatigue fracture mode. In the absence of an environmental influence (helium, vacuum and oxygen), a single power law ($\Delta K^{4.0}$) is correlated with {111} slip plane cracking. In hydrogen producing salt water (NaCl) and pure water vapor, accelerated two slope FCG behavior is associated with brittle {100} cracking and subgrain boundary cracking (SGC); characterized by two power laws (for NaCl, $\Delta K^{5.1}$ and $\Delta K^{2.7}$). The damaging effect of water vapor in moist air is presumably reduced by the presence of oxygen[2], resulting in reduced fatigue crack growth rates and multiple slope "plateau" behavior shown in Figure 11. Multiple slopes ($\Delta K^{5.1}$, $\Delta K^{1.5}$ and $\Delta K^{3.7}$) are associated with varying proportions of crystallographic {100} cracking, SGC and increased levels of inert {111} slip plane cracking.

The complex environmental fatigue crack growth behavior observed for alloy 2090 is explained in terms of a hydrogen embrittlement model[38]. Multi-sloped log da/dN - log ΔK behavior is produced by crack tip process zone hydrogen - microstructure interactions. During environmental fatigue, mobile dislocations transport adsorbed crack tip hydrogen to microstructural sinks, hydrogenating the cyclic plastic zone, and thus forming an embrittled process zone ahead of the growing fatigue crack. The rate of environmental fatigue crack growth (da/dN_{ENV}) in alloy 2090 is semiquantatively modeled by the ΔK dependent rates and proportions of each cracking mode (Θ_i) according to:

$$da/dN_{Moist\ Air} = \Theta_{\{111\}}(3\times10^{-9})\Delta K^{4.0} + \Theta_{\{100\}}(1\times10^{-8})\Delta K^{5.1} + \Theta_{SGC}(2\times10^{-7})\Delta K^{2.4} \quad (1)$$

The exponents are derived based on the plastic strain range dependencies of discontinuous crack advance over a distance (Δa) and the number of load cycles (ΔN) required to hydrogenate the process zone for each damage mechanism (fracture mode). Further research is required to independently predict the absolute values of the exponents and the preexponential coefficients. Based on empirical determinations, the environmental FCP relationship (equation 1) can be written for alloy 2090 in moist air, salt water and inert environments:

$$da/dN_{Moist\ Air} = \Theta_{\{111\}}(3\times10^{-9})\Delta K^{4.0} + \Theta_{\{100\}}(1\times10^{-8})\Delta K^{5.1} + \Theta_{SGC}(2\times10^{-7})\Delta K^{2.4} \quad (2)$$

$$da/dN_{Anodic\ NaCl} = \Theta_{\{100\}}(1.7\times10^{-7})\Delta K^{5.1} + \Theta_{SGC}(7\times10^{-7})\Delta K^{2.7} \quad (3)$$

$$da/dN_{Inert} = \Theta_{\{111\}}(3\times10^{-9})\Delta K^{4.0} \qquad \text{where } \Theta_{\{111\}} = 1.0 \quad (4)$$

Θ_i values, from fractographic analyses for each

[2] Oxygen may form a protective surface film that inhibits crack tip hydrogen embrittlement[24].

cracking mode, are in good agreement with these equations.

The model prediction, shown in Figure 11 for moist air, explains the effect of important variables, e.g., ΔK, environment chemistry and microstructure, on the environmentally induced "plateau" fatigue crack growth behavior exhibited by Al-Li-Cu alloys.

CONCLUDING REMARKS

Research over the past decade has led to the development of light weight/high strength Al-Li alloys whose environmental fatigue crack growth characteristics are superior to 7000 series and comparable to 2000 series aluminum alloys. The fatigue crack growth behavior of these advanced aluminum alloys in moist air and salt water is related to complex crack wake closure effects and crack tip environmental damage mechanisms. The effect of closure and environment are pronounced on near threshold da/dN; a regime where data are limited and further micromechanical and chemical understanding is needed. A detailed understanding of these complex phenomenon will result in the further development and the innovative damage tolerant application of these advanced materials.

REFERENCES

1. "Corrosion Control For Aircraft", AC 43-4A, FAA Advisory Circular, Washington, D.C., July 25, 1991.

2. Wei, R.P and Gangloff, R.P.: in Fracture Mechanics: Perspective and Directions, ASTM STP 1020, R.P Wei and R.P. Gangloff, eds., ASTM, Philadelphia, PA, (1989) 233-264.

3. "Aluminum-Lithium Alloys", Proc. of the I Intl. Conf. on Al-Li Alloys, T.H. Sanders, Jr. and E.A. Starke, Jr., eds., TMA-AIME, Warrendale, PA, (1981).

4. "Aluminum-Lithium Alloys II", Proc. of the II Intl. Conf. on Al-Li Alloys, C. Baker, P.J. Gregson, S.J. Harris and C.J. Peel, eds., Institute of Metals, London, U.K., (1986).

5. "4th International Aluminum-Lithium Conference", C. Champier, B. Dubost, D. Miannay and L. Sabetay, eds., J. de Phys. Coll., Vol. C3:9, Les Editions de Physique, FR (1989).

6. "Aluminum-Lithium Alloys V", Proc. of the V Intl. Conf. on Al-Li Alloys, T.H. Sanders, Jr. and E.A. Starke, Jr., eds., Materials and Component Engineeing Publications Ltd, U.K. (1989).

7. Sanders, T.H., Jr., and Starke, E.A., Jr.,: Acta Metall., Vol. 30, (1982) 927-935.

8. Venkateswara Rao, K.T., Yu, W. and Ritchie, R.O., Metall. Trans. A, Vol. 19A, (1988) 549-561.

9. Ruch, W., Jata, K. and Starke, E.A., Jr., Fatigue 84, C.J. Bewers, ed., West Midlands, UK, (1984) 145-157.

10. Venkateswara Rao, K.T. and Ritchie, R.O., Mater. Sci. Tech., Vol. 5, (1989) 882-895.

11. Venkateswara Rao, K.T., Yu, W. and Ritchie, R.O., Metall. Trans. A, Vol. 19A, (1988) 563-569.

12. Venkateswara Rao, K.T. and Ritchie, R.O., Mater. Sci. Tech., Vol. 5, (1989) 896-907.

13. "Mechanics of Fatigue Crack Closure", J.C. Newman, Jr. and Wolf Elber, eds., ASTM, Philadelphia, PA, (1988).

14. Suresh, S. and Ritchie, R.O., in Fatigue Crack Growth Threshold Concepts, D.L. Davidson and S. Suresh, eds., TMS-AIME, Warrendale, PA, (1984) 227-261.

15. "Small Fatigue Cracks", R.O. Ritchie and J. Lankford, eds., TMS-AIME, Warrendale, PA, (1986).

16. Piascik, R.S., "Intrinsic Damage Mechanisms for Environmental Fatigue Crack Propagation in Al-Li-Cu Alloys", PhD. Dissertation, University of Virginia, (1989).

17. Newman, J.C., Jr. and Edwards, P.R., " Short-Crack Growth Behavior in An Aluminum Alloy-An AGARD Cooperative Test Programme", AGARD-R-732, (1988).

18. "Short-Crack Growth Behavior in Various Aircraft Materials", P.R. Edwards and J.C. Newman, Jr., eds., AGARD-R-767, (1990).

19. Lankford, J. and Davidson, D.L., in Reference 15, 51-71.

20. Petit, J. and Zeghloul, A., in Environmental Assisted Cracking: Science and Engineering, W. Barry Lisagor, Thomas W. Crooker and Brian n. Leis, eds., STP 1049, ASTM, Philadelphia, PA, (1990) 334-346.

21. Gangloff, R.P., Metall. Trans. A., Vol. 16A (1985) 953-969.

22. Turnbull, A., Matls. Sci. Tech., Vol.1, (1985) 700-710.

23. Turnbull, A. and Ferriss, D.H., in Corrosion Chemistry Within Pits, Crevices and

Cracks, A. Turnbull, ed., HMSO, London, UK, (1987) 397-421.

24. Piascik, R.S. and Gangloff, R.P., Metall. Trans. A., Vol. 22A, (1991) 2415-2428.

25. Herman, W.A., Hertzberg, R.W. and Jaccard, R., J. Fat. and Frac. on Engr. Matls. and Struc., Vol. 11, (1988) 303-320.

26. Ritchie, R.O. and Yu, W., in Ref. 15, 167-189.

27. Donald, J.K. "Closure Measurement Techniques", Presented at the ASTM E24.04 Research Task Group Meeting, Atlanta, GA, (1988).

28. Zaiken, E. and Ritchie, R.O., Engr. Fract. Mech., Vol. 22, No. 1, (1985) 35-46.

29. James, M.R., Scripta Met., Vol. 21, (1987) 783-788.

30. Venkateswara Rao, K.T. and Ritchie, R.O., Acta. Metall., Vol. 36, No. 10, (1988) 2849-2862.

31. Vasudevan, A.K. and Bretz, P.E., in Fatigue Crack Growth Threshold Concepts, D.L. Davidson and S. Suresh, eds., TMS-AIME, Warrendale, PA, (1979) 205-243.

32. Venkateswara Rao, K.T., Bucci, R.J., Jata, K.V. and Ritchie, R.O., J. of Matls. Sci. and Engr., Vol. A141, (1991) 39-48.

33. Tintillier, R., Yang, H.S., Ranganathan, N. and Petit, J., J. De Physique, Vol. C3, (1987) 777-783.

34. Wei, R.P., Pao, P.S., Hart, R.G. and Simmons, G.W., Metall. Trans. A, Vol. 11A, (1980) 151-158.

35. Shih, T.H. and Wei, R.P., Engr. Fract. Mech., Vol. 18, (1983) 827-837.

36. Gao, M., Pao P.S. and Wei, R.P., Metall. Trans. A, Vol. 19A, (1988) 1739-1750.

37 Piascik, R.S. and Gangloff, R.P., "Environmental Fatigue of an Al-Li-Cu Alloy: Part II-Microscopic Hydrogen Cracking Processes", NASA TM-107620, 1992.

38. Piascik, R.S. and Gangloff, R.P., "Environmental Fatigue of an Al-Li-Cu Alloy: Part III-Modeling of Crack tip Hydrogen Damage", NASA TM-107619, 1992.

39. Gangloff, R.P., in Environment Induced Cracking of Metals, R.P. Gangloff and M.B. Ives, eds., NACE, Houston, TX, (1990) 55-109.

40. Peters, M., Bachmann, V. and Welpmann, K, J. De Physique, Vol. C3, (1987) 785-971.

Table 1 Typical Chemical Composition and Mechanical Properties of Commercially Available Al-Li-X Alloys[3-6]

Alloy	Li	Cu	Mg	Zn	Zr	Yield Str. (MPa)	Ult. Str. (MPa)
2090 T8	1.9-2.6	2.4-3.0	0.0-0.25	---	0.08-0.15	550	590
2091 T8	1.7-2.3	1.8-2.5	1.1-1.9	0.25	0.04-0.16	425	480
2091 T351	---	---	---	---	---	370	450
8090 T8	2.2-2.7	1.0-1.6	0.6-1.3	---	0.04-0.16	480	535
8090 T351	---	---	---	---	---	225	350
8091 T8	2.4-2.8	1.6-2.2	0.5	1.2	---	535	580
8091 T351	---	---	---	---	---	310	415

Table 2 Environmental Fatigue Fracture Modes in Alloy 2090

Environment	Low ΔK ≤2 MPa√m	Moderate ΔK 3-7 MPa√m	High ΔK ≥10 MPa√m	Comment
Vac/He/O_2	{111}	{111}	{111}	$\Delta K^{4.0}$
Moist Air	{100}	{100} SGC {111}	SGC {111}	$\Delta K^{5.1}$ LowΔK $\Delta K^{1.5}$ ModΔK $\Delta K^{3.7}$HighΔK
Water Vapor	{100}	SGC	SGC {111}	---- LowΔK $\Delta K^{2.4}$ ModΔK $\Delta K^{2.4}$HighΔK
NaCl (anodic)	{100}	SGC	SGC {111}	$\Delta K^{5.1}$ LowΔK $\Delta K^{2.7}$ ModΔK $\Delta K^{2.7}$HighΔK

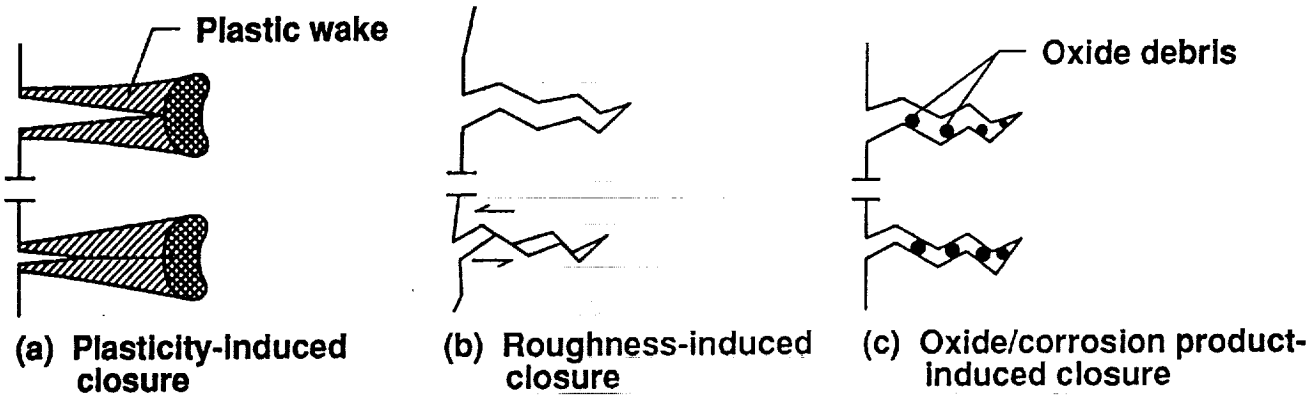

Figure 1. A schematic showing three mechanisms of crack closure[14].

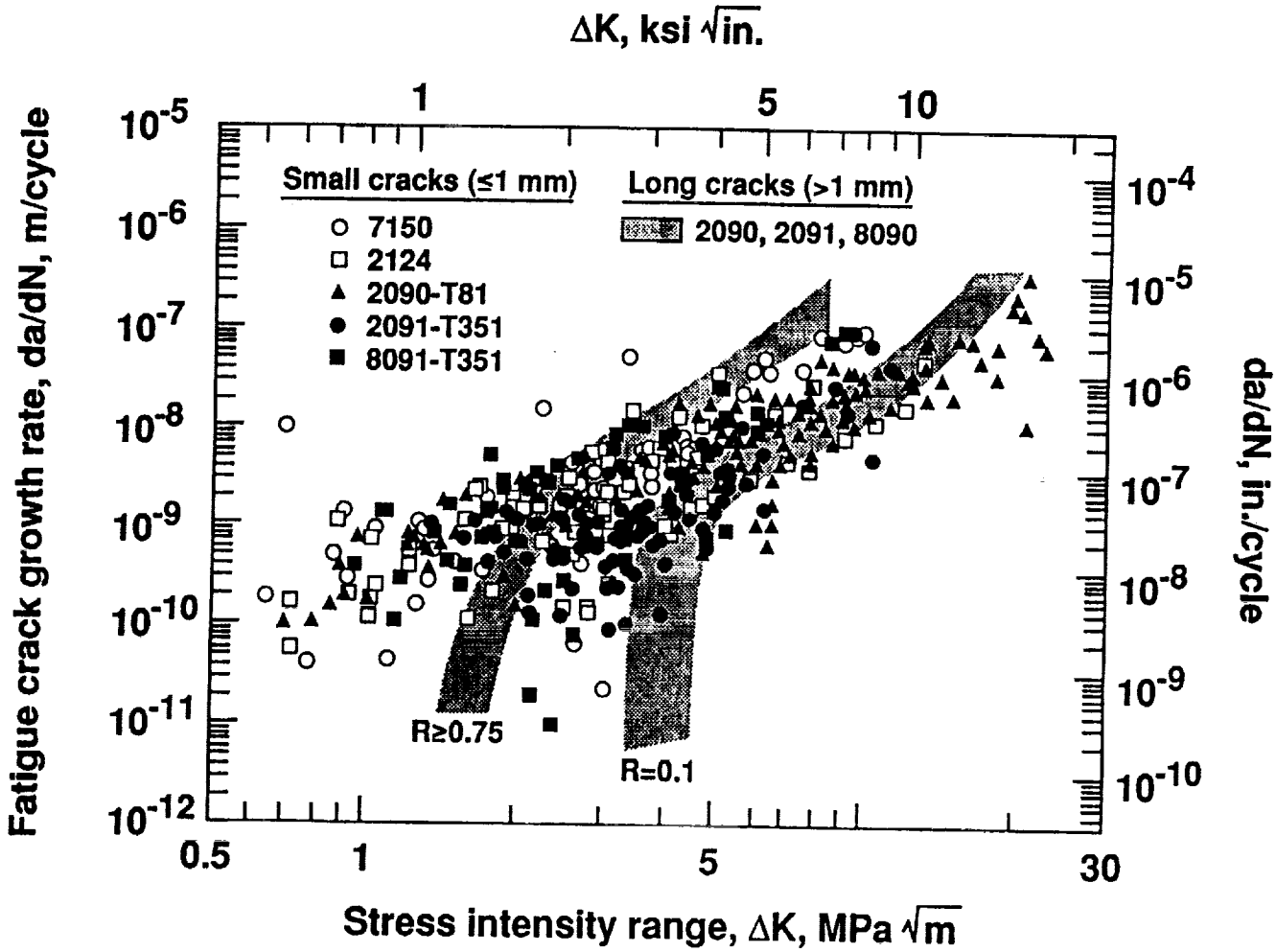

Figure 2. A comparison of long crack (high and low R) and small fatigue crack growth behavior in Al-Li and conventional high strength aluminum alloys[12,16].

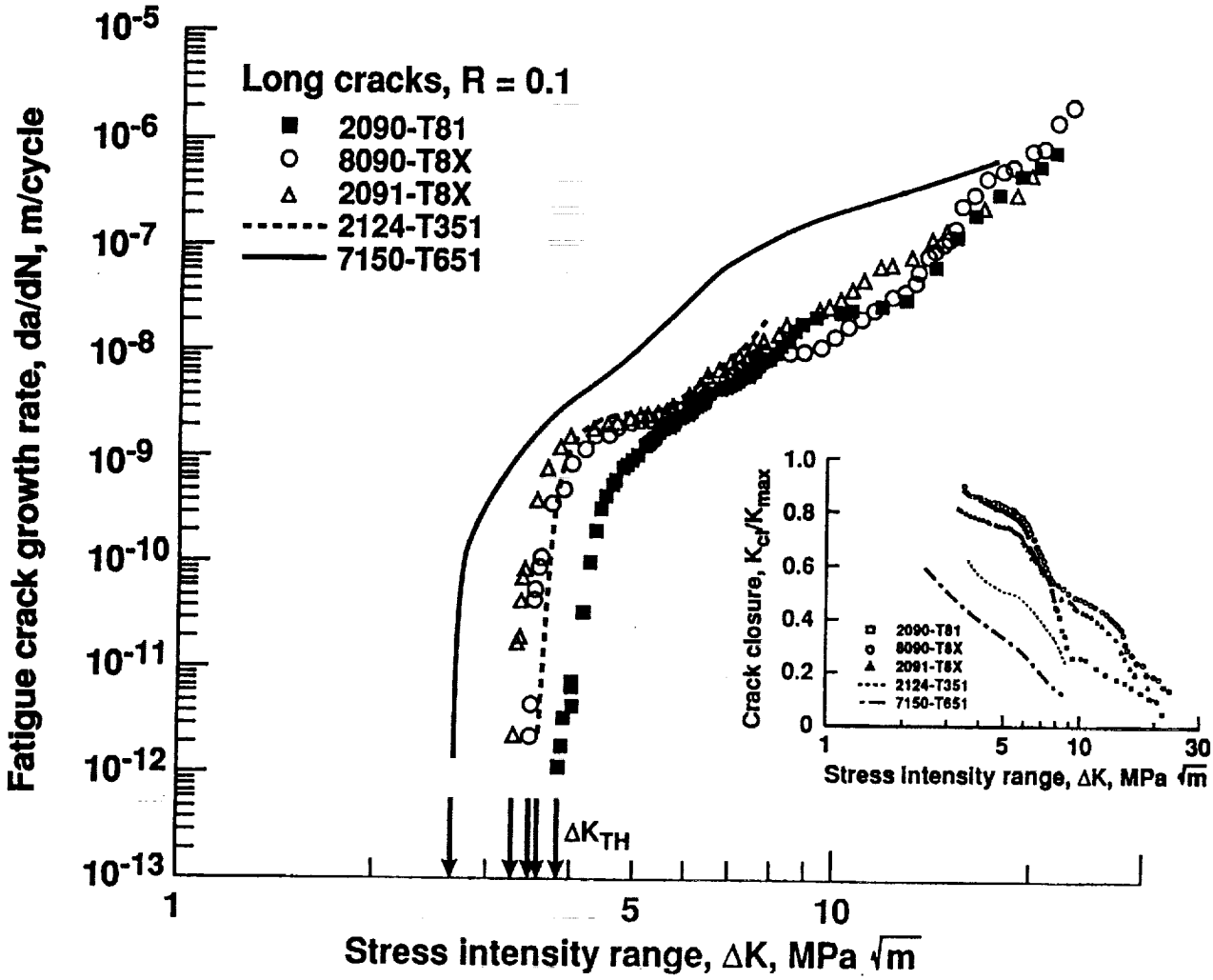

Figure 3. A comparison of long crack growth rates and closure levels in Al-Li and conventional high strength aluminum alloys at low R[8].

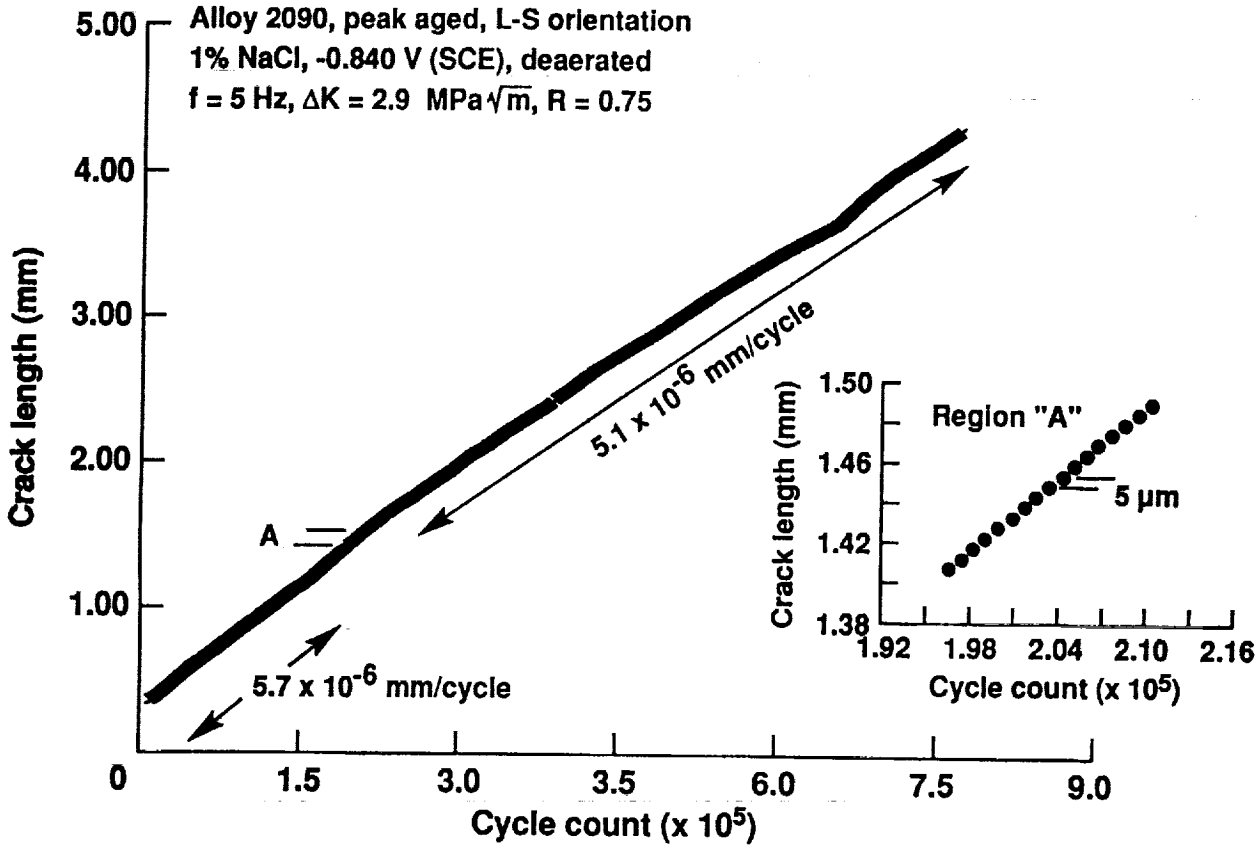

Figure 4. The effect of crack length on fatigue crack growth rate in salt water. Crack length resolution is less than 5 μm; averaged over the entire specimen thickness.

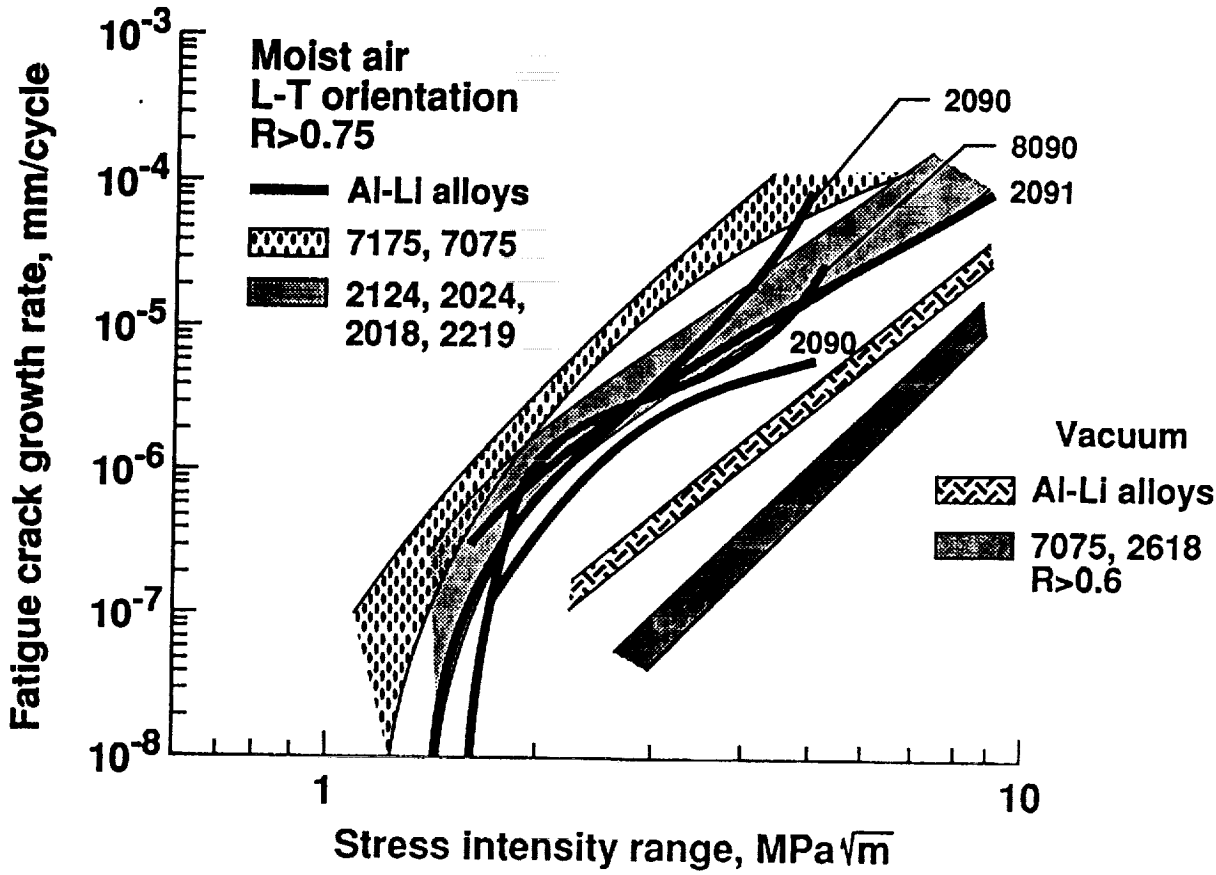

Figure 5. A comparison of the fatigue crack growth characteristics of Al-Li and conventional 2000 and 7000 series aluminum alloys in moist air and vacuum[16,24-33].

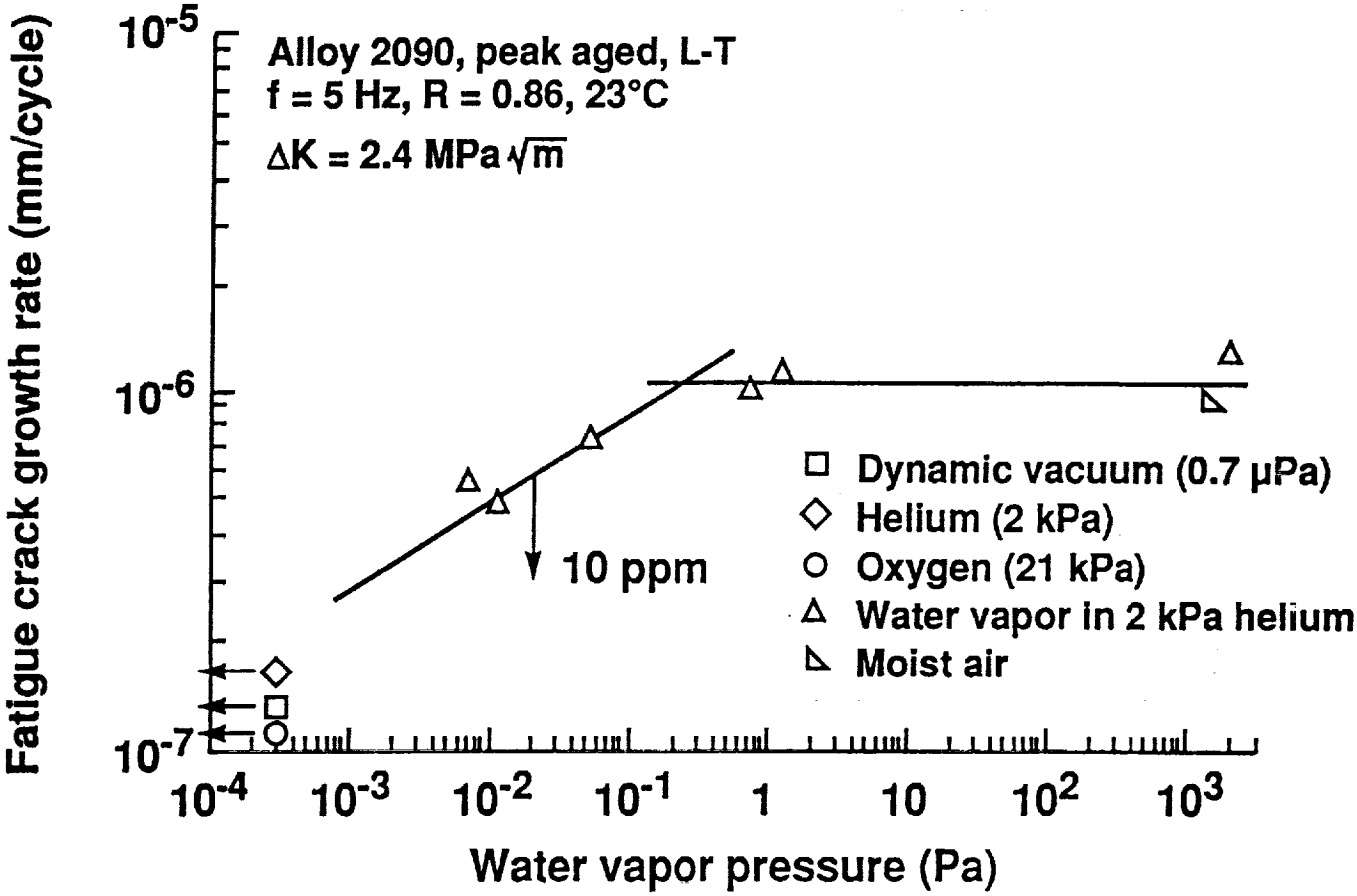

Figure 6. The effect of water vapor on near threshold fatigue da/dN in alloy 2090.

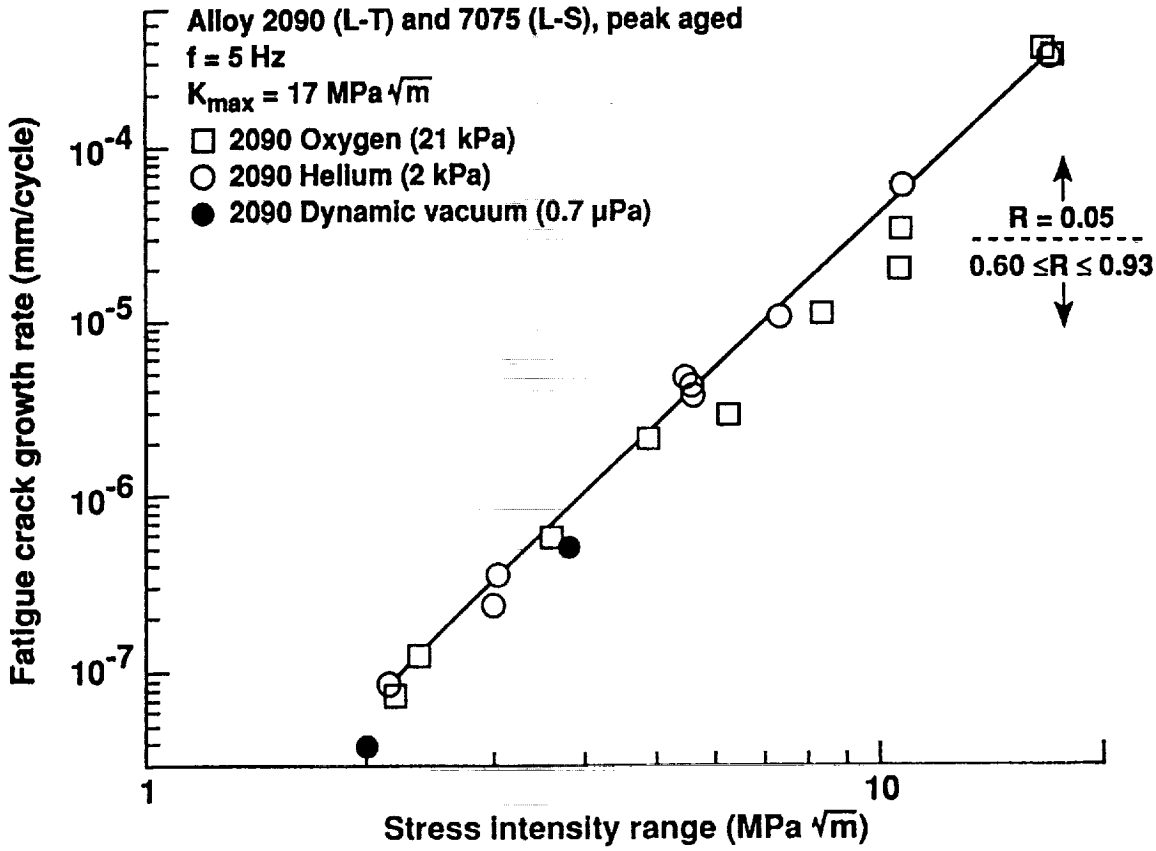

Figure 7. A comparison of the alloy 2090 fatigue crack growth rates in purified oxygen, helium and vacuum.

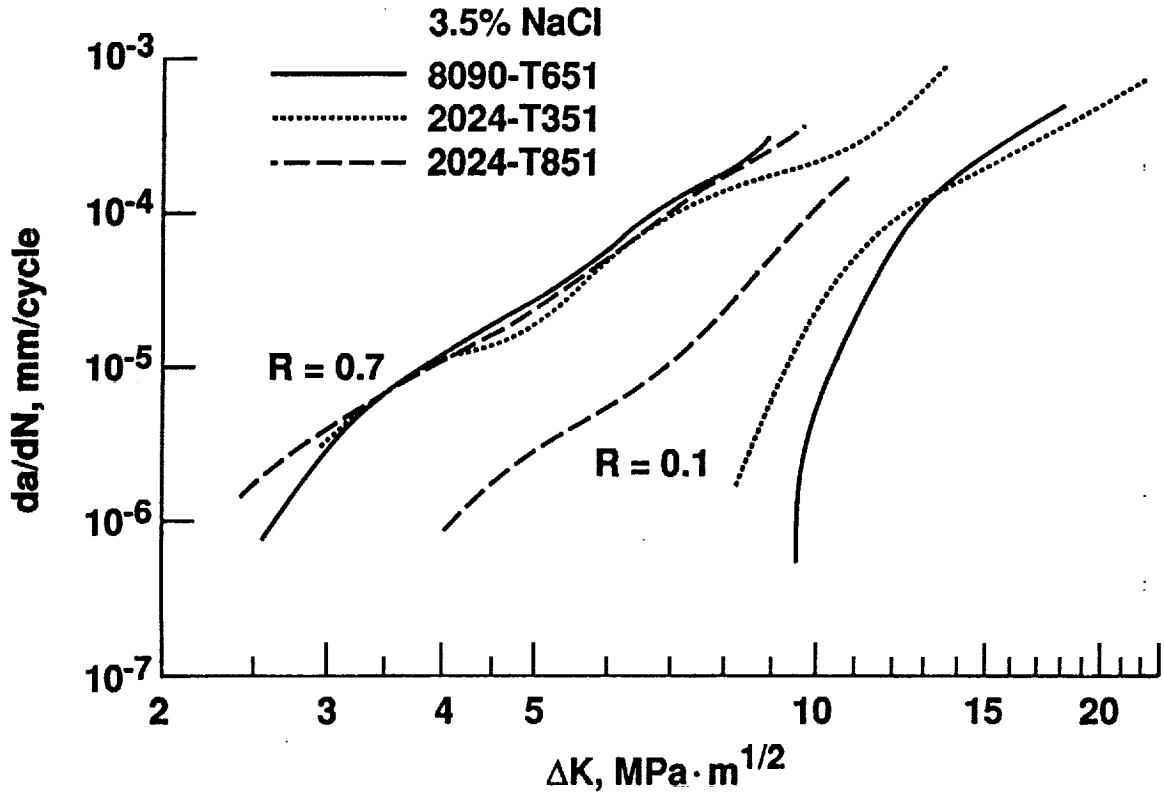

Figure 8. A comparison of the corrosion fatigue crack growth characteristics of alloys 8090 and 2024 in salt water environment[40].

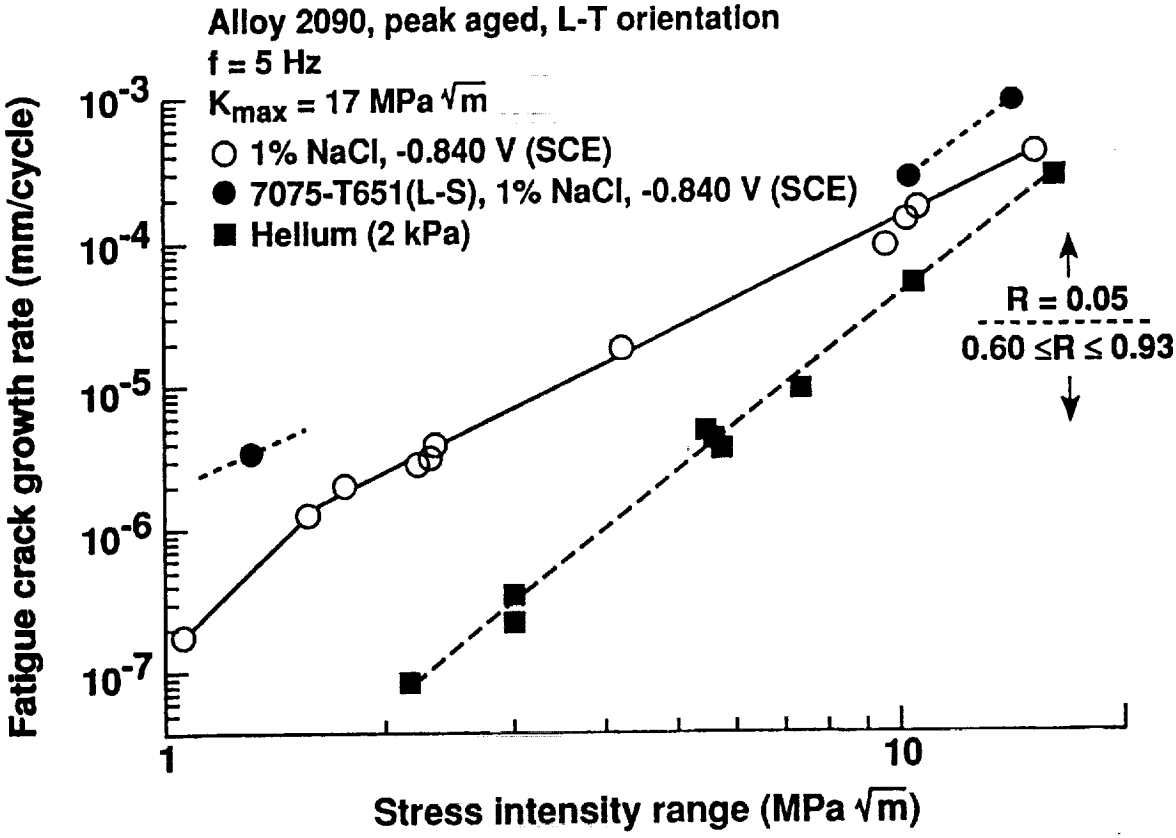

Figure 9. A comparison of the fatigue crack growth characteristics of alloys 2090 and 7075 in salt water (-0.850 V_{SCE}) and alloy 2090 inert helium.

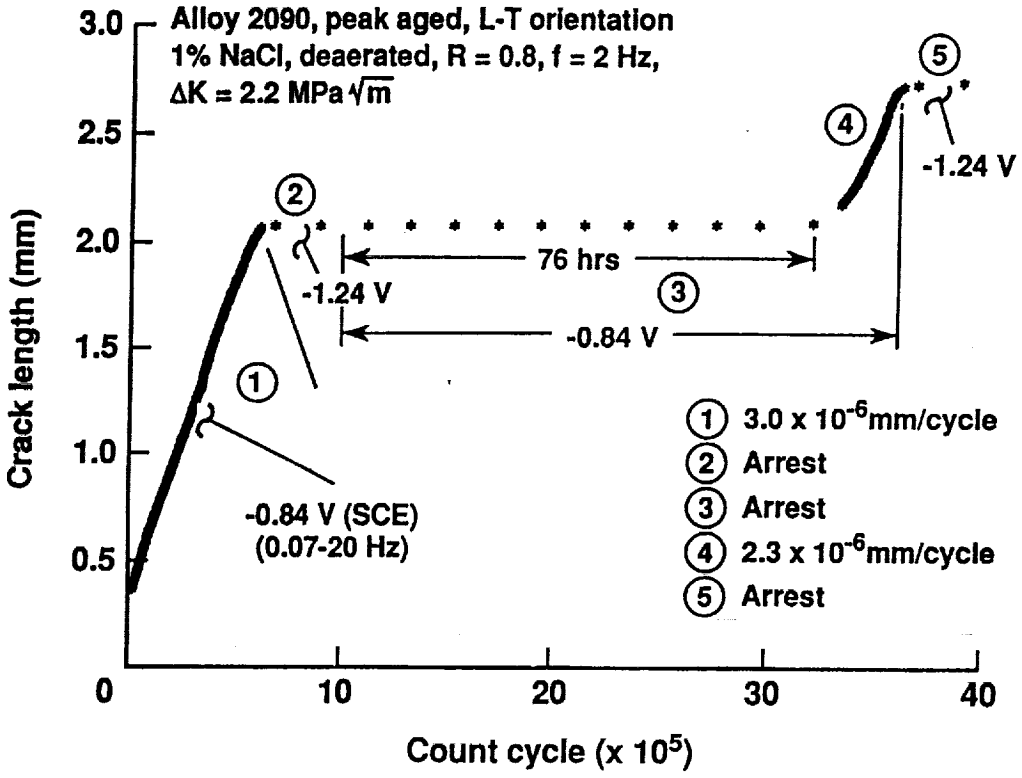

Figure 10. The effect of anodic and cathodic electrochemical potential on the near threshold fatigue crack growth rate of alloy 2090 in salt water.

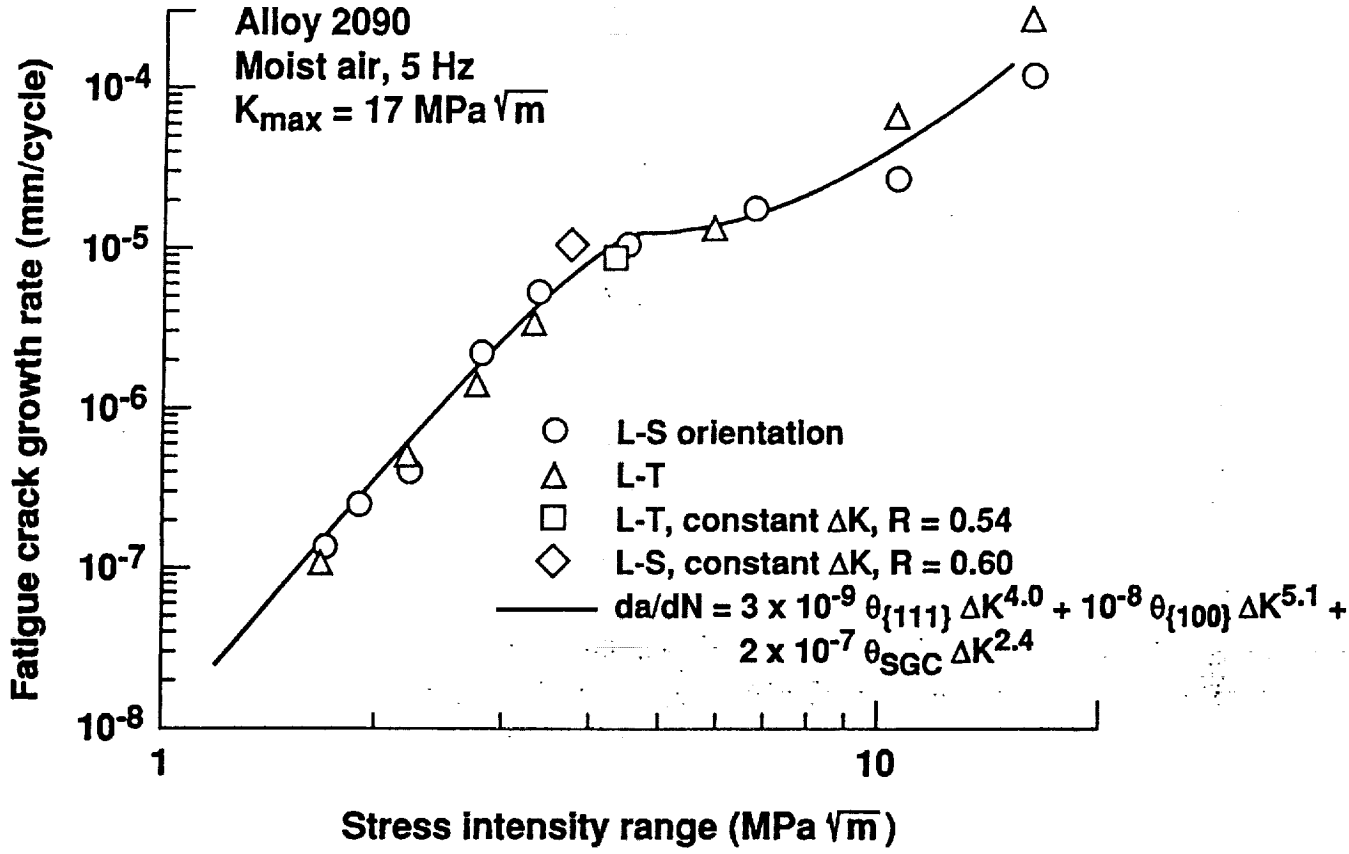

Figure 11. A comparison of measured and predicted log da/dN-log ΔK of "plateau" behavior for alloy 2090 in moist air.

REPORT DOCUMENTATION PAGE

Form Approved
OMB No. 0704-0188

1. AGENCY USE ONLY *(Leave blank)*	2. REPORT DATE	3. REPORT TYPE AND DATES COVERED
	July 1992	Technical Memorandum

4. TITLE AND SUBTITLE
Environmental Fatigue in Aluminum-Lithium Alloys

5. FUNDING NUMBERS
WU 538-02-10-01

6. AUTHOR(S)
Robert S. Piascik

7. PERFORMING ORGANIZATION NAME(S) AND ADDRESS(ES)
NASA Langley Research Center
Hampton, VA 23665-5225

8. PERFORMING ORGANIZATION REPORT NUMBER

9. SPONSORING / MONITORING AGENCY NAME(S) AND ADDRESS(ES)
National Aeronautics and Space Administration
Washington, DC 20546-0001

10. SPONSORING / MONITORING AGENCY REPORT NUMBER
NASA TM-107640

11. SUPPLEMENTARY NOTES

12a. DISTRIBUTION / AVAILABILITY STATEMENT
Unclassified - Unlimited

Subject Category 39

12b. DISTRIBUTION CODE

13. ABSTRACT *(Maximum 200 words)*

Aluminum-lithium alloys exhibit similar environmental fatigue crack growth characteristics compared to conventional 2000 series alloys and are more resistant to environmental fatigue compared to 7000 series alloys. The superior fatigue crack growth behavior of Al-Li alloys 2090, 2091, 8090, and 8091 is due to crack closure caused by tortuous crack path morphology and crack surface corrosion products. At high R and reduced closure, chemical environment effects are pronounced resulting in accelerated near threshold da/dN. The beneficial effects of crack closure are minimized for small cracks resulting in rapid growth rates. Limited data suggest that the "chemically small crack" effect, observed in other alloy system, is not pronounced in Al-Li alloys. Modeling of environmental fatigue in Al-Li-Cu alloys related accelerated fatigue crack growth in moist air and salt water to hydrogen embrittlement.

14. SUBJECT TERMS	15. NUMBER OF PAGES
Environmental fatigue; Aluminum lithium; Corrosion; Crack growth; Small crack	26
	16. PRICE CODE: A03

17. SECURITY CLASSIFICATION OF REPORT	18. SECURITY CLASSIFICATION OF THIS PAGE	19. SECURITY CLASSIFICATION OF ABSTRACT	20. LIMITATION OF ABSTRACT
Unclassified	Unclassified		